

Use of clicks resembling those of the Atlantic bottlenose dolphin (*Tursiops truncatus*) to improve target discrimination in bubbly water with biased pulse summation sonar

G.H. Chua P.R. White T.G. Leighton

Institute of Sound and Vibration Research, University of Southampton, Southampton SO17 1BJ, UK
E-mail: tgl@soton.ac.uk

Abstract: Dolphins are known to outperform man-made sonar in detecting and classifying targets in a shallow water environment where the returned signal is dominated by clutter in the vicinity of targets. During target interrogation, some species (such as the Atlantic bottlenose dolphin, *Tursiops truncatus*) emit trains of clicks. Each click can be modelled as consisting of two distinct down-chirping components over differing frequency bands. This study proposes a processing scheme called biased pulse summation sonar (BiaPSS) by which such trains can be interpreted to enhance target detection and reduce clutter in bubbly water, provided that the animal changes the amplitude of the clicks within the click train. A theoretical study is carried out using two dolphin-like clicks of different amplitude to determine the efficacy of such a pulse train in target discrimination in a bubble-filled environment. By adding and subtracting the responses from the two similar pulses, which are identical except that one has twice the amplitude of the other, the linear backscatter contribution from the target (e.g. a fish) can be discriminated from the non-linear backscattered reverberation (e.g. bubbles). For the bubble population used, the detection rate of the linear target using the pulse pair is showed to outperform the 'standard sonar' processing.

1 Introduction

Odontocetes (toothed whales) routinely produce pulsed sounds, which many studies have shown to be used for echolocation [1, 2]. The deliberate production by dolphins of bubble nets suggested that their echolocation may function well in bubbly water that would confound man-made sonar [3–5], an observation supported by the outstanding sonar performance of such animals in shallow waters. A sonar scheme – twin inverted pulse sonar (TWIPS) – which exploited the fact that bubbles would scatter closely spaced pairs of equal-amplitude pulses non-linearly, while other targets would not, was developed and tested successfully at sea [6, 7]. However, TWIPS worked because consecutive pulses had inverted phase, and the only pulses resembling these to be found in odontocetes have been recorded to date at amplitudes too low to be of use in such a processing scheme [7, 8]. Such recordings, of double or multiple pulses of equal amplitudes, have been documented from odontocetes such as from the genus *Cephalorhynchus* [9–11] and the *Phocoenidae* family [12, 13], but it is not clear if these multi-pulses are the result of surface and bottom reflections [14] or if they were directly generated at source by the animals [8, 11, 15]. Of course, the animals could make use of the second pulse of a pair in a multistatic mode even if they did not generate it [7, 8]. Regardless of whether the animal or the boundaries are the

source of the multiple pulses, given that the amplitudes appear to be too low for TWIPS, their purpose (if any) has not been determined [8].

However, it is well known that odontocetes, like the Atlantic bottlenose dolphin (*Tursiops truncatus*), emit sequences of pulses (a click train) when interrogating a target. Each pulse can have an amplitude, which is sufficient to scatter non-linearly from nearby oceanic bubble populations (while relatively low amplitudes can generate non-linear scattering in single resonant bubbles [16, 17], the broad size distribution present in the ocean requires greater insonification amplitudes to generate significant non-linear scatter from the population as a whole [7, 18]). These echolocation pulses take the form of broadband, short duration acoustic 'clicks'. Their performance in detecting and classifying targets, particularly in shallow water environments where the returned signal will usually be dominated by the scatter from the wave-generated bubble clouds if these are close to the target, is widely accepted to be superior to man-made sonar [19]. During target interrogation, there is considerable variation in the power and frequency of the dolphin clicks [1, 20–22]. The hypothesis that two dolphin-like clicks of different amplitude can be combined to improve target discrimination in a bubble-filled environment is tested in this paper.

The paper first investigates the theoretical responses for bubbles of different radii when subjected to a pair of pulses

that are identical except for having different amplitude. This information is then incorporated into a simulation of the response of a bubble cloud which contains a linear target. The signal returned by the bubble cloud is then calculated, and subsequently processed with the intention of discriminating the presence of a linearly scattering object from the bubble cloud that surrounds it. In addition to target discrimination, a further test is carried out to evaluate the performance of the use of such pulse pairs for linear target detection in a bubble-filled environment using a receiver operating characteristics (ROC) curve.

1.1 Theory

It is common for a dolphin to emit multiple pulses during target interrogation. This may be for the orthodox purpose of monitoring changes in a target, relative motion between target and source, or for insonifying different aspects of a target. However, this paper will investigate if it can further be used in clutter reduction or target discrimination. As a form of simplification, it is assumed that a first pulse, $c_1(t)$, of duration T , is followed by a second similar pulse, $c_2(t)$, of different amplitude. The response from a pulse excitation of a target that scatters linearly can be represented by $y_1(t) = h(t) * c_1(t) = \int_{\mathbb{R}} h(t-t')c_1(t')dt'$ where $h(t)$ is the impulse response of the system. If $c_2(t)$ is greater than $c_1(t)$ by a factor of G , and used as the new excitation, the response $y_2(t)$ is then given by $y_2(t) = h(t) * c_2(t) = Gy_1(t)$.

A matched filter is commonly used in sonar systems [23]. Assuming the matched filter is scaled such that its overall gain is unity, then denoting the outputs of the matched filter for $y_k(t)$ as $Y_k(t)$, where $k = 1, 2$, it follows that $Y_2(t) = GY_1(t)$. Therefore the subtraction of $GY_1(t)$ from $Y_2(t)$, which will be termed P_- in this paper, is zero for a linear scatter (not just the steady-state linear scatter [24] but also linear scatter associated with ring-up [25] and ring-down [18]). For non-linear scatterers P_- will, in general, give a non-zero value (including non-linear steady-state and non-linear ring-up/down [26, 27]). This is because for a non-linear system, the scattering from a pulse of different amplitude does not scale with the linear gain G .

The addition of $Y_2(t)$ and $GY_1(t)$, referred to as P_+ in this paper, tends to enhance the linear components of the scattered signal relative to the non-linear ones. Such processing will not lead to the complete removal of non-linear components, but only serve to partially suppress them.

The processing scheme for the linear target enhancement and non-linear scatterer enhancement by this biased pulse summation sonar (BiaPSS) is shown in Fig. 1.

2 Methods

Dolphins echolocate by emitting high-intensity broadband acoustic pulses in a directional beam and detecting echoes reflected from objects in their environment. There are numerous echolocation studies on the Atlantic bottlenose dolphin that indicate that such signals are of short duration (50–80 μ s), high intensity (up to 230 dB re 1 μ Pa peak-to-peak) and broadband [1, 2, 12]. The dolphin-like click used here is based on a double down-chirp structure and reflects the frequency bandwidth of bottlenose dolphin pulses [1, 20, 22].

For the study carried out here, each pulse is approximately 60 μ s in duration and consists of two chirps with nominal frequency band of 30–84 kHz and 76–130 kHz. The higher frequency chirp is delayed by 10 μ s relative to the lower frequency chirp. This model is based on the one proposed by Capus *et al.* [20]. The time and frequency domain representations of the dolphin-like pulse used is shown in Fig. 2. The frequency bandwidth of the pulse corresponds to a bubble resonant radius of approximately 25–110 μ m at the sea surface: although larger bubbles are generated immediately under breaking waves [28, 29], these tend to be removed from the water column by buoyancy and fragmentation, so that the background population is dominated by these smaller bubbles [7, 30, 31]. In the pair of pulses used in the simulation, the amplitude of the second pulse is 50% of that of the first pulse (the exact gain is not critical). A nominal value of 50% is chosen based on the work of Houser *et al.* [22]. In that study, two free-swimming dolphins were found to vary the source level of echolocation clicks during target acquisition with the

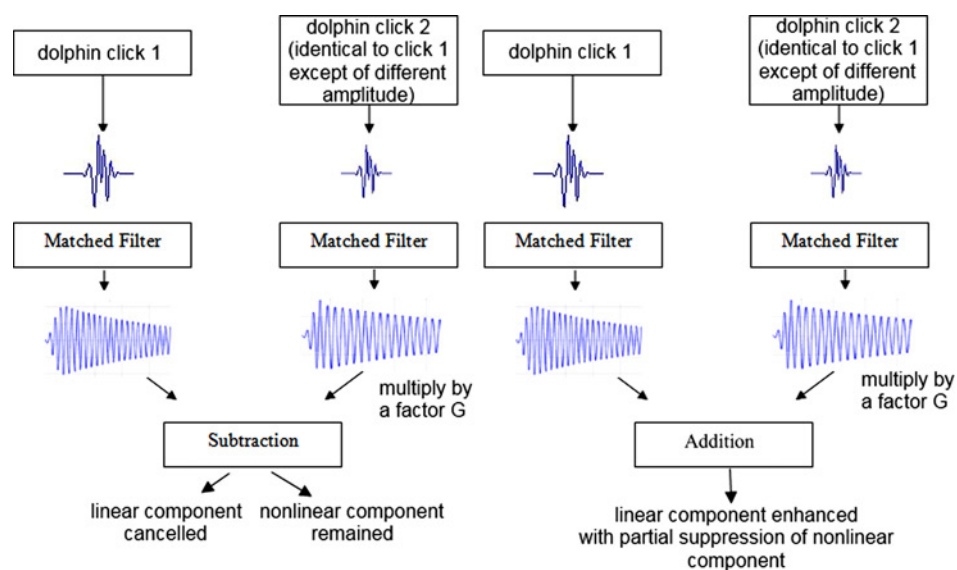


Fig. 1 Processing scheme by which the echoes from a pair of dolphin-like pulses of different amplitude are processed to enhance/cancel the non-linear/linear components of the scattering through weighted subtraction and addition of the scattering. The magnitude of the first pulse is greater than that of the second pulse by a factor of G

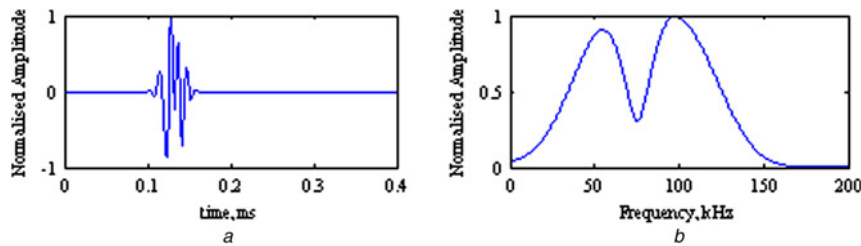


Fig. 2 Pulse used in the simulation presented in

- a Time-domain
- b Frequency-domain with peak-to-peak SPL of approximately 228 dB re 1 μ Pa

difference in level ranging from approximately 1–6 dB. Although there are suggestions of physiological constraints that coarsely couple both source level and frequency content in animals like the bottlenose dolphin and false killer whale (*Pseudorca crassidens*) [32], the model used here is further simplified with the assumption that the increase in source level is independent of peak frequency.

The theoretical responses for bubbles of different radii when subjected to a pair of pulses of different amplitudes are first computed using the non-linear Keller–Miksis [33] model implemented in MATLAB[®]. This model assumes spherical oscillations of a single bubble in water and extends the Rayleigh–Plesset model by considering a compressible medium with a constant speed of sound.

$$\begin{aligned} & R\ddot{R}\left(1 - \frac{\dot{R}}{c}\right) + \frac{3}{2}\dot{R}^2\left(1 - \frac{\dot{R}}{3c}\right) \\ &= \left(1 + \frac{\dot{R}}{c}\right)\frac{1}{\rho}\left[p_L(t) - P_\infty - p\left(t + \frac{R}{c}\right)\right] + \frac{R}{\rho c}\frac{dp_L(t)}{dt} \end{aligned} \quad (1)$$

where R is the instantaneous radius of the bubble, with \dot{R} and \ddot{R} being its first and second temporal derivatives, respectively, ρ is the density of the liquid, c is the speed of sound in the liquid, p_∞ is the static pressure in the liquid from the bubble, usually equal to the sum of the atmosphere and hydrostatic pressures, $p(t)$ is the drawing pressure signal and $p_L(t)$ is the liquid pressure on the external side of the bubble wall, which is related to the bubble gas pressure $p_g(t)$ via the vapour pressure p_v with the surface tension and liquid shear viscosity denoted by σ and μ , respectively [34]

$$p_g(t) = p_L(R, t) + \frac{2\sigma}{R} + 4\mu\frac{\dot{R}}{R} - p_v \quad (2)$$

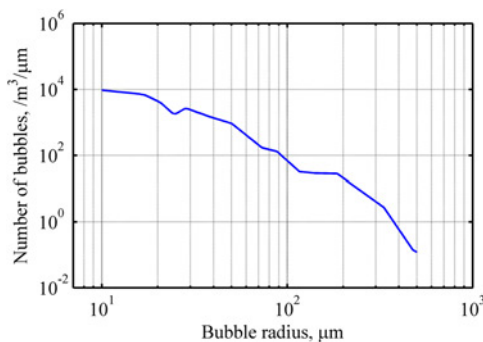


Fig. 3 Bubble population used expressed in number of bubbles per cubic metre per micron bin width in bubble radius

Equation (1) was solved using a variable step length Runge–Kutta method. The scattered pressure at a given distance from each bubble was then calculated from the radius and velocity of the bubble surface for each time point [34].

These responses are incorporated into a sonar simulation model to assess the performance of such a pulse pair in the classification and detection of a linear target in a bubble-filled environment. The simulation uses the theoretical responses of representative bubbles, characterising a bubble size bin encompassing bubbles of similar radii using (1). The three-dimensional volume of liquid is divided into spatial cells into which the bubble population, and the target, may be placed. The responses from all the bubbles from that volume are calculated by convolving the bin-representative bubble response with the bubble population for that volume. A bubble population consistent with historic ocean measurements [30, 31, 35–38] is used in the simulation and is shown in Fig. 3. The void fraction of the cloud used is of the order of $10^{-5}\%$ which is within the range of void fractions of the ambient bubble population in open ocean [39], and not so high that multiple scattering between bubbles need to be considered [18, 40]. The void fraction used is more typical of the ambient bubble population left over after successive

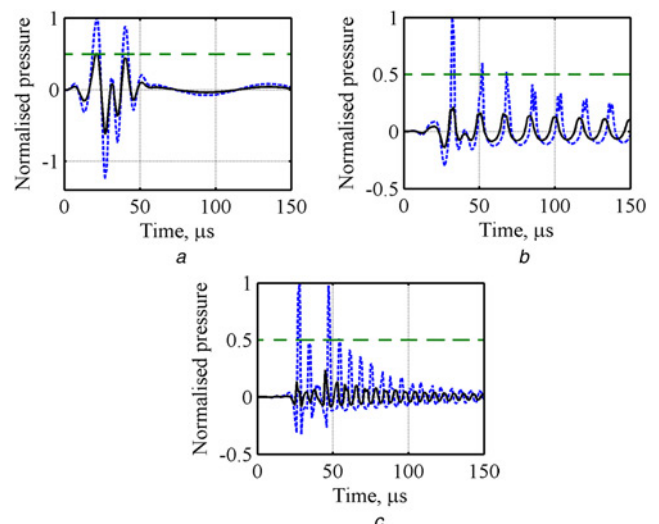


Fig. 4 Bubble response to the first pulse (denoted by the dotted line) and the second pulse (denoted by the solid line) normalised by the maximum positive pressure of the bubble response because of the first pulse. The horizontal dashed line shows the 50% mark of the peak amplitude of the first pulse. The bubble radius in

- a is 250 μ m
- b is 50 μ m
- c is 20 μ m

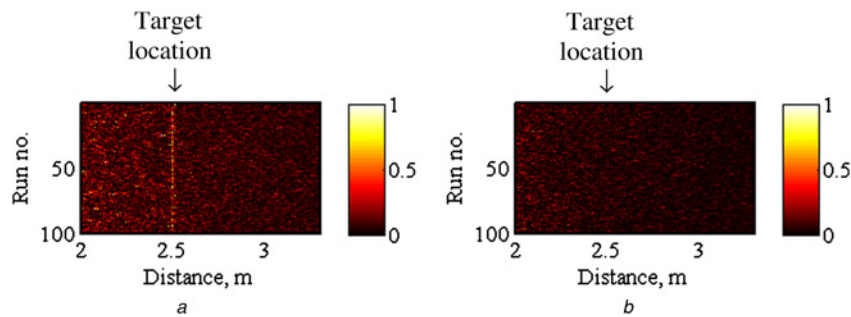


Fig. 5 The target is located at 2.5 m. Each colour scale is linearly scaled and has been normalised to a common value of 4.5×10^8 for easy comparison Simulation of target ($TS = -35$ dB) in a bubble-filled environment with the image plots of

a P_+
b P_-

breaking waves than it is of the population in a breaking wave [38]. In the simulation, for the pulses within the same pulse pair, the bubble cloud is unchanged. Between runs, the bubble cloud is allowed to evolve, with the restriction that the overall bubble population does not change. The target is assumed to be an instantaneous linear scatterer with a target strength of -35 dB. Pulse attenuation (which is readily demonstrated from bubble clouds [41], but which in littoral waters at these frequencies will come from suspended sediments [42–44] etc.) is not included to maintain a manageable computational load. The smoothed envelopes of the return signals (over consecutive runs) are processed as described in Fig. 1, and for display purposes are then stacked (with amplitude represented by colour, as defined in the colour bar), forming image plots for comparison. The image plots show the repeatability of the test as the bubble cloud evolves. For the image plots shown, 100 separate runs have been stacked.

3 Results

By comparing the responses of a scatterer from a pair of pulses of different amplitude (through weighted addition and subtraction), discrimination between linear and non-linear scatterers can occur. To illustrate this, consider Fig. 4, which shows the normalised responses of a bubble of different radius when excited by two pulses of different amplitudes. In Figs. 4a and c, the resonant frequency of

the bubble is outside the frequency bandwidth of the pulse. For the case of Fig. 4a, the resonant frequency of the bubble is lower than the frequency bandwidth of the input pulse, whereas in Fig. 4c, the resonant frequency is above the frequency bandwidth of the pulse. In the case shown in Fig. 4a, the bubble cannot respond rapidly enough to generate a non-linear response and behaves like a linear scatterer [45]. Bubbles which are sufficiently smaller that their resonant frequencies are higher than the frequency of the driving pulse (Fig. 4c), can still respond rapidly to the compressive or expansive half-cycles, and hence can still undergo non-linear pulsations, albeit to a lesser extent than those bubbles within the frequency of the driving pulse [45]. This means that the responses of these bubbles will also not scale with the amplitude of the input pulse. Likewise, when the resonant frequency of the bubble is within the frequency bandwidth of the pulse as in Fig. 4b, the amplitude of the response of the bubble does not scale with the amplitude of the input pulse.

The plots in Fig. 5 show how a linear and non-linear scatterer can be discriminated using a pair of pulses of different amplitude when a linear target is placed within a bubble-filled environment. Fig. 5a shows (on a linear colour scale) the results obtained when a pulse pair (of which the second pulse has an amplitude that is half of the first) were added, so highlighting the presence of the target. By subtracting the response from the first pulse with the correctly scaled responses from the second pulse, the linear scatters are removed as observed in Fig. 5b. By comparing

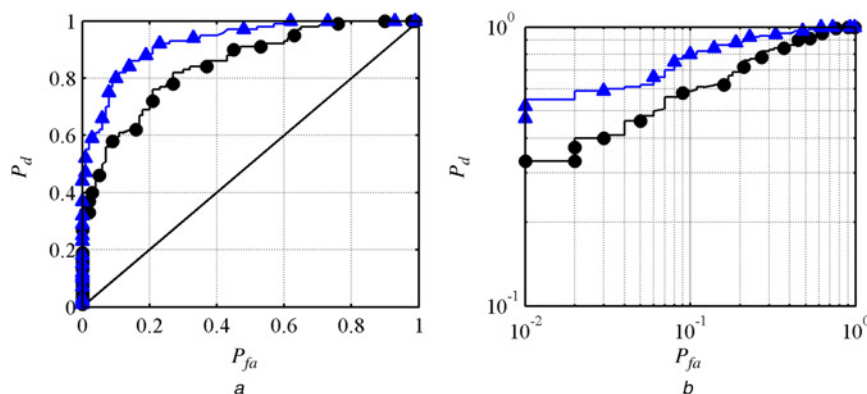


Fig. 6 ROC curves of standard sonar processing compared with P_+ for case shown in Fig. 5 where the solid circles are the ROC curve of the former and the solid triangles represent the ROC curve of the latter P_d is the probability of detection while P_{fa} is the probability of false alarm.

a Linear scale is used for both axes, while in
b Logarithmic scale is used for both axes

the image plots of the sum and difference of the responses from the pulse pair, discrimination between linear and non-linear scatterers can take place.

A further test is carried out to determine if the use of the sum of the responses from the pulse pair, P_+ , can improve linear target detection compared to 'standard sonar' processing. In this context, standard sonar processing consists of averaging the smoothed envelopes of the match-filtered responses from the pulse pair. This is compared with the processing scheme for the enhancement of linear scatterers (shown in Fig. 1) where the match-filtered signal from the pulse pair is first linearly added before obtaining the smoothed envelopes. A ROC curve [46] comparing the relative performance of the two processing is shown in Fig. 6. The ROC curve is generated using the distribution of the backscattered response in the region around the target position in the target absent and target present cases. The region selected corresponds to approximately one pulse length centred on the target location. In Fig. 6a, linear axes are used for the ROC curve while in (b), logarithmic axes are used to display a more useful range of probability of detection and probability of false alarm. The sum of the responses from a pair of pulses of different amplitude gives a probability of detection of 46% before giving a single false alarm (i.e. on the $P_{fa} = 0$ axis), compared to a probability of detection of 27% for standard sonar processing before giving a single false alarm. Depending on the scenario, even small levels of false alarm can be costly (e.g. a false alarm in mine detection could entail closure of a sea route and deployment of divers).

4 Discussion

Fig. 5 shows that by using a pair of pulses of different amplitude, discrimination between linear and non-linear scatterers can occur. Fig. 5a illustrates the performance of P_+ and shows the presence of the bubbles and the linear target. These bubbles were mostly the larger bubbles, which are not excited to high-enough amplitude for non-linear pulsations to occur. The corresponding results of P_- (Fig. 5b) shows only the non-linear backscattered reverberation (from the bubble cloud). Hence, by comparing both image plots, classification of linear and non-linear backscatter can occur.

The ROC curves in Fig. 6 also show that the sum of the responses from the two pulses of different amplitude gives a higher probability of detection before giving a single false alarm when compared to the standard sonar processing. This can be attributed to the scattering from the bubbles, which varied as the amplitude of input pulse halved. The enhancement in linear target scattering suggests that the scattering from the bubbles tend to be incoherent. Hence, the linear sum of the signal responses resulted in reduced backscattered reverberation from the bubble, and an increased scatter from the linear target. This translated to a higher probability of detection in the ROC curve.

Although the results presented here suggest the use of a pair of dolphin-like pulses of different amplitude allow for discrimination between linear and non-linear scatterers and can potentially improve the detection of a linear target in a bubble-filled environment, the authors are not aware of evidence which shows that dolphin can process pulses of different amplitude in the same manner, despite some studies suggesting that dolphins can combine multiple echoes for target detection and estimation [47, 48].

In general, the effectiveness of the signals with different amplitude increases when a greater proportion of the bubble population scatter non-linearly, and it is easier for the bubble to scatter non-linearly if the pulse frequency is close to the bubble resonant frequency. It is also intriguing to note that the frequency bandwidth of the dolphin 'clicks' coincides with the resonant frequencies of bubble sizes, which are most numerous in typical oceanic conditions.

5 Conclusion

The simulations suggest that the use of a pair of dolphin-like pulses of different amplitude can discriminate between linear and non-linear scatterers using BiaPSS. For the bubble population used in the simulation, the detection performance of the linear target in the bubble-filled environment is also shown to outperform standard sonar processing in the ROC curves.

6 References

- 1 Au, W.W.L.: 'The sonar of dolphins' (Springer-Verlag, New York, 1993)
- 2 Au, W.W.L., Nachtigall, P.E.: 'Acoustics of echolocating dolphins and small whales', *Mar. Freshwater Behav. Physiol.*, 1997, **29**, (1), pp. 127–162
- 3 Leighton, T.G.: 'From seas to surgeries, from babbling brooks to baby scans: the acoustics of gas bubbles in liquids', *Int. J. Mod. Phys. B*, 2004, **18**, (25), pp. 3267–3314
- 4 Leighton, T.G.: 'Nonlinear bubble dynamics and the effects on propagation through near-surface bubble layers'. in Porter, M.B., Siderius, M., Kuperman, W. (Eds.): 'High Frequency Ocean Acoustics: High Frequency Ocean Acoustics Conf.' (American Institute of Physics, Melville, New York, 2004), pp. 180–193
- 5 Leighton, T.G., Finfer, D.C., White, P.R.: 'Bubble acoustics: what can we learn from cetaceans about contrast enhancement?'. Proc. IEEE Int. Ultrasonics Symp., Rotterdam, 2005 18th–21st sept. 2005, pp. 964–973
- 6 Leighton, T.G., Finfer, D.C., Chua, G.H., White, P.R., Dix, J.: 'Clutter suppression and classification using twin inverted pulse sonar in ship wake', *J. Acoust. Soc. Am.*, 2011, **13**, (5), pp. 3431–3437
- 7 Leighton, T.G., Finfer, D.C., White, P.R., Chua, G.H., Dix, J.K.: 'Clutter suppression and classification using twin inverted pulse sonar (TWIPS)', *Proc. R. Soc. A*, 2010, **466**, pp. 3453–3478
- 8 Finfer, D.C., White, P.R., Leighton, T.G.: 'The occurrence of double-pulses from odontocetes who are primarily restricted to shallow water', IET Radar, Sonar & Navigation doi: 10.1049/rsn.2011.0348
- 9 Dawson, S.M.: 'The high-frequency sounds of free-ranging Hector's dolphin, *Cephalorhynchus hectori*', *Rep. Int. Whal. Commun. Spec. Issue*, 1988, **9**, pp. 339–341
- 10 Evans, W.E., Aubrey, F.T., Hackbarth, H.: 'High frequency pulse produced by free ranging Commerson's dolphin (*Cephalorhynchus commersonii*) compared to those of phocoenids', *Rep. Int. Whal. Commun. Spec. Issue*, 1988, **9**, pp. 173–181
- 11 Gotz, T., Antunes, R., Heinrich, S.: 'Echolocation clicks of free-ranging Chilean dolphins (*Cephalorhynchus eutropia*)', *J. Acoust. Soc. Am.*, 2010, **128**, (2), pp. 563–566
- 12 Kamminga, C., Wiersma, H.: 'Investigations on cetacean sonar II. Acoustical similarities and differences in odontocete sonar signals', *Aquat. Mammals*, 1981, **8**, pp. 41–62
- 13 Li, S., Wang, K., Wang, D., Akamatsu, T.: 'Echolocation signals of the free-ranging Yangtze finless porpoise (*Neophocaena phocaenoides asiaeorientalis*)', *J. Acoust. Soc. Am.*, 2005, **117**, (5), pp. 3288–3296
- 14 Li, S., Wang, K., Wang, D., Akamatsu, T.: 'Origin of the double- and multi-pulse structure of echolocation signals in Yangtze finless porpoise (*Neophocaena phocaenoides asiaeorientalis*)', *J. Acoust. Soc. Am.*, 2005, **118**, (6), pp. 3934–3940
- 15 Lammers, M.O., Castellote, L.: 'The beluga whale produces two pulses to form its sonar signal', *Biol. Lett.*, 2009, **5**, pp. 297–301
- 16 Leighton, T.G., Phelps, A.D., Ramble, D.G., Sharpe, D.A.: 'Comparison of the abilities of eight acoustic techniques to detect and size a single bubble', *Ultrasonics*, 1996, **34**, (6), pp. 661–667
- 17 Leighton, T.G., Ramble, D.G., Phelps, A.D.: 'The detection of tethered and rising bubbles using multiple acoustic techniques', *J. Acoust. Soc. Am.*, 1997, **101**, (5), pp. 2626–2635

- 18 Leighton, T.G., Meers, S.D., White, P.R.: 'Propagation through nonlinear time-dependent bubble clouds and the estimation of bubble populations from measured acoustic characteristics', *Proc. R. Soc. A*, 2004, **460**, pp. 2521–2550
- 19 Au, W.W.L.: 'The dolphin sonar: excellent capabilities in spite of some mediocre properties', in Porter, M.B., Siderius, M., Kuperman, W. (Eds.): 'High frequency ocean acoustics' (AIP Conf. Proc., American Institute of physics, New York, 2004) pp. 247–259.
- 20 Capus, C., Pailhas, Y., Brown, K., Lane, D.M.: 'Bio-inspired wideband sonar signals based on observations of the bottlenose dolphin (*Tursiops truncatus*)', *J. Acoust. Soc. Am.*, 2007, **121**, (1), pp. 594–604
- 21 Houser, D.S., Helweg, D.A., Moore, P.W.: 'Classification of dolphin echolocation clicks by energy and frequency distribution', *J. Acoust. Soc. Am.*, 1999, **106**, (3), pp. 1579–1585
- 22 Houser, D.S., Martin, S.W., Bauer, E.J., *et al.*: 'Echolocation characteristics of free-swimming bottlenose dolphins during object detection and identification', *J. Acoust. Soc. Am.*, 2005, **117**, (4), pp. 2308–2317
- 23 Burdic, W.S.: 'Underwater acoustic system analysis', in Oppenheim, A.V. (Ed.): "Prentice-Hall signal processing series" (Prentice-Hall, Inc., Englewood Cliffs, NJ, 1984)
- 24 Ainslie, M.A., Leighton, T.G.: 'Near resonant bubble acoustic cross-section corrections, including examples from oceanography, volcanology, and biomedical ultrasound', *J. Acoust. Soc. Am.*, 2009, **126**, (5), pp. 2163–2175
- 25 Clarke, J.W.L., Leighton, T.G.: 'A method for estimating time-dependent acoustic cross-sections of bubbles and bubble clouds prior to the steady state', *J. Acoust. Soc. Am.*, 2000, **107**, (4), pp. 1922–1929
- 26 Leighton, T.G.: 'Transient excitation of insonated bubbles', *Ultrasonics*, 1989, **27**, (1), pp. 50–53
- 27 Leighton, T.G., Walton, A.J., Field, J.E.: 'High-speed photography of transient excitation', *Ultrasonics*, 1989, **27**, pp. 370–373
- 28 Phelps, A.D., Ramble, D.G., Leighton, T.G.: 'The use of a combination frequency technique to measure the surf zone bubble population', *J. Acoust. Soc. Am.*, 1997, **101**, (4), pp. 1981–1989
- 29 Deane, G.B., Stokes, M.D.: 'Air entrainment processes and bubble size distributions in the surf zone', *J. Phy. Oceanogr.*, 1999, **29**, (7), pp. 1393–1403
- 30 Breitz, N., Medwin, H.: 'Instrumentation for *in situ* acoustical measurements of bubble spectra under breaking waves', *J. Acoust. Soc. Am.*, 1989, **86**, (2), pp. 739–743
- 31 Farmer, D.M., Vagle, S.: 'Waveguide propagation of ambient sound in the ocean-surface bubble layer', *J. Acoust. Soc. Am.*, 1989, **86**, (5), pp. 1897–1908
- 32 Au, W.W.L., Pawloski, J.L., Nachtigall, P.E., Blonz, M., Gisner, R.: 'Echolocation signals and transmission beam pattern of a false killer whale (*Pseudorca crassidens*)', *J. Acoust. Soc. Am.*, 1995, **98**, pp. 51–59
- 33 Keller, J.B., Miksis, M.: 'Bubble oscillations of large-amplitude', *J. Acoust. Soc. Am.*, 1980, **68**, (2), pp. 628–633
- 34 Leighton, T.G.: 'The acoustic bubble' (Academic Press, London, 1994)
- 35 Johnson, B.D., Cooke, R.C.: 'Bubble populations and spectra in coastal waters – photographic approach', *J. Geophys. Res.-Oceans Atmos.*, 1979, **84**, (NC7), pp. 3761–3766
- 36 Medwin, H.: 'In situ acoustic measurements of bubble populations in coastal ocean waters', *J. Geophys. Res.*, 1970, **75**, (3), pp. 599–611
- 37 Meers, S.D., Leighton, T.G., Clarke, J.W.L., Heald, G.J., Dumbrell, H.A., White, P.R.: 'The importance of bubble ring-up and pulse length in estimating the bubble distribution from propagation measurements'. In Leighton, T.G., Heald, G.J., Griffiths, H.D., Griffiths, G., 'Acoustical oceanography' (Proceedings of the Institute of Acoustics, **23** (2), Bath University Press, 2001), pp. 235–241
- 38 Phelps, A.D., Leighton, T.G.: 'Oceanic bubble population measurements using a buoy-deployed combination frequency technique', *IEEE J. Oceanic Eng.*, 1998, **23**, (4), pp. 400–410
- 39 Stokes, M.D., Deane, G.B.: 'A new optical instrument for the study of bubbles at high void fractions within breaking waves', *IEEE J. Oceanic Eng.*, 1999, **24**, (3), pp. 300–311
- 40 Kargl, S.G.: 'Effective medium approach to linear acoustics in bubbly liquids', *J. Acoust. Soc. Am.*, 2002, **111**, (1), pp. 168–173
- 41 Leighton, T.G., Jiang, J., Baik, K.: 'Demonstration comparing sound wave attenuation inside pipes containing bubbly water and water droplet fog', *J. Acoust. Soc. Am.*, 2011 **131**, (3), Pt. 2, pp. 2413–2421
- 42 Brown, N.R., Leighton, T.G., Richards, S.D., Heathershaw, A.D.: 'Measurement of viscous sound absorption at 50–150 kHz in a model turbid environment', *J. Acoust. Soc. Am.*, 1998, **104**, (4), pp. 2114–2120
- 43 Richards, S.D., Leighton, T.G., Brown, N.R.: 'Visco-inertial absorption in dilute suspensions of irregular particles', *Proc. R. Soc. A*, 2003, **459**, (2038), pp. 2153–2167
- 44 Richards, S.D., Leighton, T.G., Brown, N.R.: 'Sound absorption by suspensions of nonspherical particles: measurements compared with predictions using various particle sizing techniques', *J. Acoust. Soc. Am.*, 2003, **114**, (4), pp. 1841–1850
- 45 Leighton, T.G.: 'What is ultrasound?', *Prog. Biophys. Mol. Biol.*, 2007, **93**, (1–3), pp. 3–83
- 46 Fawcett, T. Hewlett Packard Laboratories., Palo Alto, USA: 'ROC graphs: notes and practical considerations for researchers'. Technical Report HPL-2003–4 Report, 2004
- 47 Dankiewicz, L.A., Helweg, D.A., Moore, P.W., Zafran, J.M.: 'Discrimination of amplitude-modulated synthetic echo trains by an echolocating bottlenose dolphin', *J. Acoust. Soc. Am.*, 2002, **112**, (4), pp. 1702–1708
- 48 Altes, R.A., Dankiewicz, L.A., Moore, P.W., Helweg, D.A.: 'Multiecho processing by an echolocating dolphin', *J. Acoust. Soc. Am.*, 2003, **114**, (2), pp. 1155–1166